

Reorientation of Anisotropy in a Square Well Quantum Hall Sample

W. Pan^{1,2}, T. Jungwirth^{3,4}, H.L. Stormer^{5,6}, D.C. Tsui¹, A. H. MacDonald³, S. M. Girvin³, L. Smrčka⁴, L.N. Pfeiffer⁵, K.W. Baldwin⁵, and K.W. West⁵

¹*Department of Electrical Engineering, Princeton University, Princeton, New Jersey 08544*

²*NHMFL, Tallahassee, Florida 32310*

³*Department of Physics, Indiana University, Bloomington, Indiana 47405*

⁴*Institute of Physics ASCR, Cukrovarnická 10, 162 00 Praha 6, Czech Republic*

⁵*Bell Labs, Lucent Technologies, Murray Hill, New Jersey 07974*

⁶*Department of Physics and Department of Applied Physics, Columbia University, New York, New York 10027*
(November 1, 2018)

We have measured magnetotransport at half-filled high Landau levels in a quantum well with two occupied electric subbands. We find resistivities that are *isotropic* in perpendicular magnetic field but become strongly *anisotropic* at $\nu = 9/2$ and $11/2$ on tilting the field. The anisotropy appears at an in-plane field, $B_{ip} \sim 2.5$ T, with the easy-current direction *parallel* to B_{ip} but rotates by 90° at $B_{ip} \sim 10$ T and points now in the same direction as in single-subband samples. This complex behavior is in quantitative agreement with theoretical calculations based on a unidirectional charge density wave state model.

A two-dimensional (2D) electron gas is an attractive system for many-body physics studies [1,2]. A particularly rich variety of phenomena associated with strong interactions among electrons appears in the regime of the fractional quantum Hall effect (FQHE) [3,4]. During much of the last decade, studies of the FQHE have focused on even-denominator Landau level filling factors [5,6] such as the compressible $\nu = 1/2$ state and the $\nu = 5/2$ incompressible quantum Hall fluid. Most recently, strongly anisotropic transport has been observed in high quality GaAs/Al_xGa_{1-x}As single heterojunctions [7–11] at filling factors $\nu = 9/2, 11/2$, etc., and in 2D hole systems [12] starting at $\nu = 5/2$. In these experiments, the magnetoresistance shows a strong peak in one current direction and a deep minimum in the perpendicular current direction. Tilting the magnetic field away from the sample normal causes the high resistance direction to change from its original orientation to the in-plane magnetic field direction.

The origin of the magnetotransport anisotropy has not been firmly established yet. The most appealing interpretation suggests that the 2D electron gas spontaneously breaks the translational symmetry by forming a unidirectional charge density wave (UCDW), as predicted by Hartree-Fock theory [13,14]. This idea has spurred much theoretical interest [15–28]. Because of uncertainty about the reliability of this Hartree-Fock prediction, there has been a special emphasis [19,20] placed on tests of its ability to explain experimental results on “stripe” orientation in tilted magnetic fields. In particular, Jungwirth et al. [19] carried out detailed many-body RPA/Hartree-Fock calculations combined with a self-consistent local-spin-density-approximation (LSDA) description of one-

particle states in experimental sample geometries. For the sample parameters of the traditional, single-interface specimens of Refs. [10,11] with a single electric subband occupied, the theory [19,20] gives stripes oriented perpendicular to the field, consistent with experiment.

A theoretical study [19] of UCDWs in parabolic quantum wells that have two subbands occupied in zero magnetic field, has predicted much more complex behavior of the UCDW state, including stripe states induced by an in-plane field and rotation of stripe orientation at critical in-plane field strengths. A comparison between theory and experiment in a geometry for which this intricate behavior occurs, constitutes an excellent test of the UCDW explanation of anisotropic transport in higher Landau levels. Since parabolic quantum wells are experimentally difficult to realize and suffer from poor mobility we, instead, chose a square well structure which is expected to exhibit similarly complex behavior, provided that more than one electric subband is occupied in zero field.

Our sample, detailed in Figure 1(c), consists of a 350Å wide GaAs quantum well bracketed between thick Al_{0.24}Ga_{0.76}As layers grown on a (100) GaAs substrate by MBE. Two Si delta-doping layers are placed symmetrically above and below the quantum well at a distance of 800Å. The specimen has a size of 5mm × 5mm and is contacted via eight indium contacts, placed symmetrically around the perimeter. The electron density is established after illuminating the sample with a red light-emitting diode at ~ 4.2 K and we measure an electron mobility of $\mu = 7 \times 10^6$ cm²/V s. The total electron density, $n = 4.6 \times 10^{11}$ cm⁻², is determined from low-field Hall data. The subband densities, $n_1 = 3.3 \times 10^{11}$ cm⁻² and $n_2 = 1.3 \times 10^{11}$ /cm⁻², are obtained by Fourier analysis of

the low-field Shubnikov-de Haas oscillation. Their values coincide with the results of our numerical self-consistent LSDA calculation. All angular-dependent measurements were carried out at $T = 40$ mK in a top-loading dilution refrigerator equipped with an *in-situ* rotator [29] placed inside a 33T resistive magnet. A low-frequency (~ 7 Hz) lock-in technique at a current $I = 10$ nA is used. We define the axis of rotation as the y -axis. Consequently, the in-plane field, B_{ip} , is along the x -axis when the sample is rotated. Therefore, R_{xx} refers to “ I parallel to B_{ip} ” and R_{yy} refers to “ I perpendicular to B_{ip} ” [30].

Figure 1(a) shows an overview of magnetoresistance at zero-tilt. The shaded region highlights the transport features around $\nu = 9/2$ and $11/2$. The integer quantum Hall effect (IQHE) states at $\nu = 1, 2, 3, \dots$ and the FQHE states at $\nu = 2/3$, etc. are clearly visible. Figure 1(b) shows the results of self-consistent LSDA calculations of Landau levels (measured from the bottom of the quantum well) in perpendicular magnetic field.

Figure 2 shows the R_{xx} and R_{yy} data for $4 < \nu < 6$ at four different tilt angles $\theta = 0^\circ, 41.2^\circ, 67.9^\circ$, and 76.2° . The tilt angle is determined using the shift of prominent QHE states, which depend only on the perpendicular magnetic field, $B_{perp} = B \times \cos\theta$.

In the absence of B_{ip} ($\theta = 0^\circ$), R_{xx} and R_{yy} show a peak at $\nu = 9/2$ and a slight dip at $\nu = 11/2$ and negligible anisotropy. The small difference in magnitude between R_{xx} and R_{yy} is probably a result of the different contacts involved in both measurements. This practically *isotropic* behavior of R_{xx} and R_{yy} is distinctively different from results [7–11] on single-subband, single-heterojunctions, where the states at $\nu = 9/2$ and $11/2$ are strongly anisotropic in the absence of B_{ip} . This lack of anisotropy in our sample has a simple interpretation. The diagram in Figure 1(b) indicates that the $\nu = 9/2$ and $11/2$ states are the $\nu = 3/2$ state of the lowest Landau level ($N=0$) in the second quantum well subband ($i=2$). The $\nu = 3/2$ state in single subband samples exhibits isotropic transport, which seems to carry over to the second subband. Yet, exceptional behavior develops on tilting the specimen.

At $\theta = 41.2^\circ$ the R_{xx} and R_{yy} traces are very different from those taken at zero field-tilt and different from each other. The $\nu = 9/2$ and $\nu = 11/2$ states are strongly anisotropic with the hard-axis perpendicular to B_{ip} (R_{yy}) and the easy-axis parallel to B_{ip} (R_{xx}). The direction of this tilt-induced anisotropy (TIA) is *rotated by 90°* as compared to the direction in traditional single-subband, single-heterojunction structures [10,11]. As the tilt angle increases further, the R_{xx} and R_{yy} traces approach each other again at $\theta \sim 67.9^\circ$ rendering the transport nearly isotropic (Figure 2(c)). Beyond this angle the anisotropy reemerges but the hard-axis and easy-axis *have traded places*, as seen in Figure 2(d).

In Figures 3(a,b) we plot R_{xx} and R_{yy} at filling factors $\nu = 9/2$ and $11/2$ versus B_{ip} . Their general behavior is

rather similar. Practically isotropic transport prevails in the range of $0 < B_{ip} < 2$ T, but there is a clear onset to anisotropy at $B_{ip} \sim 2.5$ T. The level of anisotropy rapidly increases, reaching its peak at $B_{ip} \sim 5.0$ T, whereupon the R_{xx} and R_{yy} values approach each other again and cross at $B_{ip} \sim 10$ T. For higher in-plane fields the transport is again anisotropic, but its direction has *rotated by 90°* . Figures 3(c,d) show the anisotropy factor, defined as $(R_{xx} - R_{yy})/(R_{xx} + R_{yy})$ and derived from the data of the panels above. They clearly depict the initially, practically isotropic behavior followed by a strong anisotropy that rotates direction by 90° at $B_{ip} \sim 10$ T. The direction of anisotropy in single-subband samples corresponds to the high B_{ip} direction in our double-subband specimen.

We now turn to the analysis of correspondence between the measured TIA and the theory based on the UCDW picture. For an infinitely narrow electron layer the effective 2D Coulomb interaction, $V(\vec{q})$, reduces to $e^{-q^2\ell^2/2}/q (L_N(q^2/2))^2 2\pi e^2\ell/\epsilon$ where $L_N(x)$ is the Laguerre polynomial, \vec{q} is the wavevector, ℓ is the magnetic length, and ϵ is the dielectric function. Starting from $N = 1$, zeros of $L_N(q^2/2)$ occur at finite $q = q^*$, producing a zero in the repulsive Hartree interaction at wave vectors where the attractive exchange interaction is strong. For the half-filled valence Landau level the corresponding UCDW state consists of alternating occupied and empty stripes of electron guiding center states with a modulation period $\approx 2\pi/q^*$.

In finite-thickness 2D systems subjected to tilted magnetic fields, the dependence of the effective interaction on wavevector magnitude q and orientation ϕ relative to the in-plane field direction can be accurately approximated [19] by $V(\vec{q}) = V_0(q) + V_2(q) \cos(2\phi)$. At $B_{ip} = 0$, the isotropic term $V_0(q)$ has a wavevector-dependence similar to that of the effective interaction in the infinitely narrow 2D layer. The corresponding curve for the valence Landau level at $\nu = 9/2$, shown in the top inset of Figure 4, has no zeros at finite q -vectors *because* the half-filled valence Landau level is the $N = 0$ state of the second subband (as shown in detail in Figure 1(b)) [31]. Hence, the UCDW state is not expected to form, consistent with the isotropic transport measured in perpendicular field.

Because of the finite thickness of the 2D system in our 350Å wide quantum well, the orbital effect of the in-plane field causes Landau levels emanating from different electric subbands to coincide, depending on the strength of B_{ip} . The in-plane field mixes electric and magnetic levels so the subband and orbit radius indices are no longer good quantum numbers. However, the effect of B_{ip} near the level (anti)crossing can sometimes be viewed approximately as a transfer of valence electrons from the lowest ($N = 0$) Landau level of the second subband to a higher ($N > 0$) Landau level of the first subband. For filling factor $\nu = 9/2$, such a circumstance occurs in our sample at $B_{ip} \approx 3$ T, as seen from the top and bottom insets

of Figure 4. Indeed, $V_0(q)$ is only slightly modified at low in-plane fields, while a clear minimum develops for $B_{ip} > 3$ T. As discussed above for the case of perpendicular magnetic field it is the minimum of the interaction energy at finite wavevector that opens the possibility for the formation of the UCDW state. The theoretical and experimental critical in-plane fields corresponding to the onset of the UCDW and TIA, respectively, are remarkably close.

The non-zero anisotropy coefficient $V_2(q)$ of the effective interaction at $B_{ip} > 0$ is responsible for the non-zero UCDW anisotropy energy E_A , defined [19] as the total Hartree-Fock energy of stripes oriented parallel with B_{ip} minus the total energy of stripes perpendicular to B_{ip} . The direction of the anisotropy results from a delicate competition between electrostatic and exchange contributions to E_A and can be determined only by an accurate calculation which takes into account details of the experimental configuration. As shown in Figure 4, the stripes align parallel with B_{ip} at low in-plane fields, consistent with the measured easy-current direction parallel with B_{ip} . The sign of the UCDW anisotropy energy changes at $B_{ip} = 10$ T which coincides with the experimental critical field for the interchange of easy and hard current axes. This theoretical discussion of the $\nu = 9/2$ state was found to apply for $\nu = 11/2$ as well.

In conclusion, we have observed complex transport behavior in a two-subband QW at half-filled high Landau levels. Both the transition to an anisotropic transport state, at finite B_{ip} , and the rotation of the direction of anisotropy by 90° at higher B_{ip} are explained quantitatively by the UCDW picture. The close agreement between complex experimental data and theoretical results leaves little doubt as to the origin of the observed transport anisotropies in high Landau levels.

We would like to thank E. Palm and T. Murphy for experimental assistance, and N. Bonesteel, R.R. Du, and K. Yang for useful discussion. A portion of this work was performed at the National High Magnetic Field Laboratory which is supported by NSF Cooperative Agreement No. DMR-9527035 and by the State of Florida. The work at Indiana University was supported by NSF grant DMR-9714055, and at the Institute of Physics ASCR by the Grant Agency of the Czech Republic under grant 202/98/0085. D.C.T. and W.P. are supported by the DOE and the NSF.

-
- [1] *The Quantum Hall Effect* edited by R.E. Prange and S.M. Girvin (Springer-Verlag, New York, 1990).
 - [2] T. Chakraborty and P. Pietiläinen, *The Fractional Quantum Hall Effect*, Springer Series in Solid State Science **85** (Springer-Verlag, New York, 1988).
 - [3] D.C. Tsui, H.L. Stormer, and A.C. Gossard, Phys. Rev. Lett. **48**, 1558 (1982).

- [4] R.B. Laughlin, Phys. Rev. Lett. **50**, 1395 (1983).
- [5] *Perspectives in Quantum Hall Effects* edited by S. Das Sarma and A. Pinczuk (Wiley, New York, 1996).
- [6] *Composite Fermions: A Unified View of the Quantum Hall Regime* edited by O. Heinonen (World Scientific, Singapore, 1998).
- [7] H.L. Stormer, R.R. Du, D.C. Tsui, L.N. Pfeiffer, and K.W. West, Bull. Amer. Phys. Soc. **38**, 235 (1993).
- [8] M. P. Lilly, K.B. Cooper, J.P. Eisenstein, L.N. Pfeiffer, and K.W. West, Phys. Rev. Lett. **82**, 394 (1999).
- [9] R.R. Du, D.C. Tsui, H.L. Stormer, L.N. Pfeiffer, K.W. Baldwin, and K.W. West, Solid State Commun. **109**, 389 (1999).
- [10] W. Pan, R.R. Du, H.L. Stormer, D.C. Tsui, L.N. Pfeiffer, K.W. Baldwin, and K.W. West, Phys. Rev. Lett. **83**, 820 (1999).
- [11] M.P. Lilly, K.B. Cooper, J.P. Eisenstein, L.N. Pfeiffer, and K.W. West, Phys. Rev. Lett. **83**, 824 (1999).
- [12] M. Shayegan, H.C. Manoharan, S.J. Papadakis, and E.P. De Poortere, Physica E, **6**, 40 (2000).
- [13] A. A. Koulakov, M. M. Fogler, and B. I. Shklovskii, Phys. Rev. Lett. **76**, 499 (1996); M.M. Fogler, A.A. Koulakov, and B.I. Shklovskii, Phys. Rev. B **54**, 1853 (1996); M.M. Fogler and A.A. Koulakov, Phys. Rev. B **55**, 9326 (1997).
- [14] R. Moessner and J. T. Chalker, Phys. Rev. B **54**, 5006 (1996).
- [15] E. Fradkin and S. A. Kivelson, Phys. Rev. B **59**, 8065 (1999).
- [16] H.A. Fertig, Phys. Rev. Lett. **82**, 3593 (1999).
- [17] E.H. Rezayi, F.D.M. Haldane, and Kun Yang, Phys. Rev. Lett. **83**, 1219 (1999).
- [18] S.H. Simon, Phys. Rev. Lett. **83**, 4223 (1999).
- [19] T. Jungwirth, A.H. MacDonald, L. Smrčka, and S.M. Girvin, Phys. Rev. B **60**, 15574 (1999).
- [20] T. Stanescu, I. Martin, and P. Phillips, Phys. Rev. Lett. **84**, 1288 (2000).
- [21] E. Fradkin, S.A. Kivelson, E. Manousakis, and K. Nho, Phys. Rev. Lett. **84**, 1982 (2000).
- [22] E.H. Rezayi and F.D.M. Haldane, cond-mat/9906137.
- [23] A.H. MacDonald and M.P.A. Fisher, Phys. Rev. B **61**, 5724 (2000).
- [24] N. Maeda, Phys. Rev. B **61**, 4766 (2000).
- [25] Yue Yu, Shi-Jie Yang, and Zhao-Bin Su, cond-mat/9909192.
- [26] F. von Oppen, B.I. Halperin, and A. Stern, Phys. Rev. Lett. **84**, 2937 (2000).
- [27] Ziqiang Wang, cond-mat/9911265.
- [28] R. Côté and H.A. Fertig, cond-mat/001169.
- [29] E.C. Palm and T.P. Murphy, Rev. Sci. Instrum. **70**, 237 (1999).
- [30] A separate experiment, where we applied B_{ip} along y -axis, gave similar results to those presented in Fig. 2 and Fig. 3.
- [31] Landau levels in perpendicular and tilted magnetic fields were calculated using the full self-consistent local-spin-density-approximation (LSDA) method. Effective 2D Coulomb interaction curves were obtained from the LSDA one-particle orbitals. The screening from electrons occupying the lower filled Landau levels was accounted for using the RPA. For details of the calculations see [19].

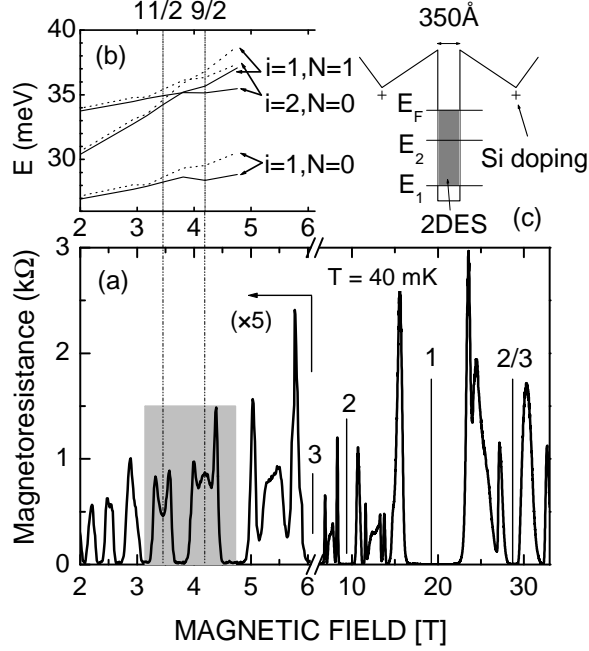


FIG. 1. (a) Overview of magnetoresistance in perpendicular magnetic field. The IQHE states ($\nu = 1, 2, 3$, etc.) and the FQHE states ($\nu = 2/3$, etc.) are marked by vertical lines. Shaded region highlights the transport features around $\nu = 9/2$ and $11/2$. (b) Self-consistent LSDA energy levels in perpendicular field. Index of electric subband (i) and Landau level (N) is shown for each energy level. Solid lines represent the spin-up state and dotted lines represent the spin-down state. (c) Structure of our quantum well sample. The well width is 350\AA . E_F , E_2 , and E_1 are the zero-field Fermi energy, second, and first subband energy level, respectively.

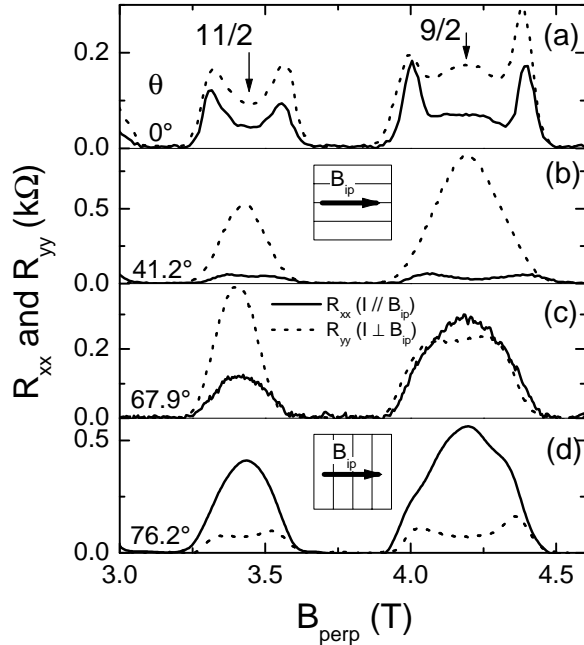


FIG. 2. Magnetoresistance R_{xx} (solid lines) and R_{yy} (dotted lines) between $4 < \nu < 6$ as a function of perpendicular magnetic field, B_{perp} , at four tilt angles, θ . The in-plane magnetic field B_{ip} is along the x -axis. Stripes in the insets of panels (b) and (d) indicate the tilt-induced anisotropy (TIA) at $\nu = 9/2$ and $11/2$.

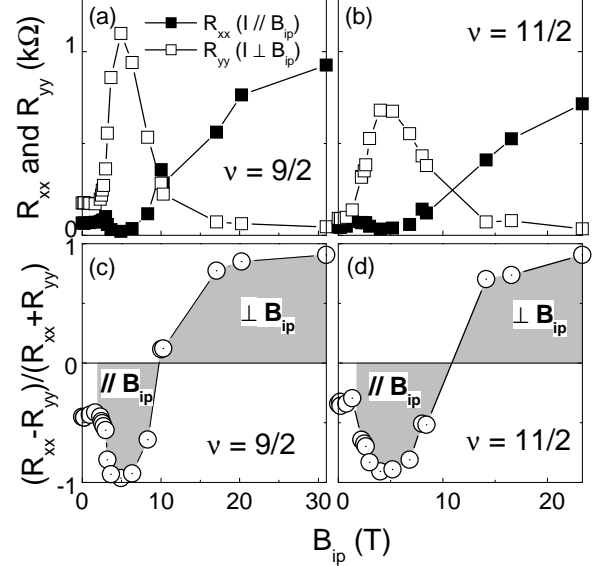


FIG. 3. Amplitude of R_{xx} (solid squares) and R_{yy} (open squares) at $\nu = 9/2$ [panel (a)] and at $\nu = 11/2$ [panel (b)] as a function of B_{ip} . Panels (c) and (d) show the anisotropy factor, defined by $(R_{xx} - R_{yy})/(R_{xx} + R_{yy})$ and derived from the data of the panels above. The shade regions represent the tilt-induced anisotropy (TIA) parallel with and perpendicular to B_{ip} , respectively.

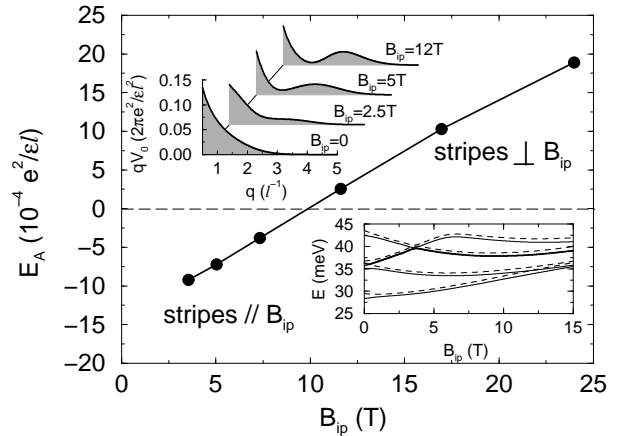


FIG. 4. Theoretical results for the $\nu = 9/2$ state. Main graph: UCDW anisotropy energy as a function of in-plane magnetic field. Top inset: the isotropic term of the effective 2D Coulomb interaction multiplied by the wavevector amplitude q at different in-plane fields. Bottom inset: self-consistent LSDA Landau levels as a function of in-plane magnetic field. Thick line is the half-filled valence Landau level.